GSA DATA REPOSITORY 2014120

Bank pull or bar push: what drives scroll-bar formation in meandering rivers?

Van de Lageweg et al.

EXTENDED METHOD SECTION

Experimental settings:

Scaling from experimental to natural bend migration rates cannot proceed from classical dimensional analysis because this assumes a priori known and fixed channel widths. Since we were interested in general mechanisms and processes rather than exact dynamic similarity with a specific prototype, we relaxed the scaling rules whilst requiring that the morphodynamic processes are similar. Three scaling requirements were fulfilled for process similarity with natural meandering gravel-bed rivers: 1) flow remained just subcritical; 2) bed sediment was mobile as bed load whilst the silt-sized silica flour acted as wash load; and 3) the coarser particles ensure hydraulically rough boundary to prevent scour holes (Van Dijk et al., 2012; Van de Lageweg et al., 2013).

Cases 1-7 were tested in a single experiment that last for 160 hrs. The experiment was conducted with a constant discharge of 1800 L/hr. Case 8 was tested during an experiment that took 120 hrs. This experiment was conducted with a hydrograph of low flow (Q = 900 L/hr) with a duration of 2.5 hr and high flow (Q = 1800 L/hr) with a duration of 0.5 hr. Sediment-feed rate was kept constant for both experiments (Q_s of 0.25 L/hr) such that neither bed aggradation nor degradation occurred. Bed and feed sediment had particle-size percentiles of $D_{10,50,90}$ = (0.30, 0.71, 2.00) mm. In case 8, 0.5 L of a weakly cohesive silt-sized silica flour (D_{50} = 32 μm) was added in the feed during high flow. We used a sediment mixture ranging from silt-sized silica flour to fine gravel, where the gravel provided sufficient flow resistance and turbulence to disrupt the viscous sublayer and keep the channel floor hydraulically rough to prevent silt deposition and unrealistic scour holes (Van Dijk et al., 2012; Van de Lageweg et al., 2013).

An initial straight channel of 0.15 m wide and 0.01 m deep was carved on a plain with a slope of 1.0×10^{-2}. Sustained perturbations at the upstream boundary maintained the dynamics so that point bars reformed even after cutoffs. The perturbation resembles a bend instability that initiates meanders, the perturbation has to be sustained as these instabilities convect in downstream direction for meandering rivers (Lanzoni and Seminara, 2006; Van Dijk et al., 2012). Van Dijk et al. (2012) showed that for experiments a minimum rate of perturbation is needed and that channel development is bounded to a maximum perturbation rate which depended on the erodibility of the banks. A sustained perturbation was obtained by the transversely moving of the inflow point with a constant rate of 10 mm/hr to an amplitude of 300 mm. Even with the perturbation we observed temporarily static bends which did not migrate in lateral direction, probably due to a lack of dynamic variations from upstream (Lanzoni et al., 2006, Van Dijk et al., 2012). Therefore, we tested the effect of bar push also on a naturally static bend, to identify if lateral bend migration could by pushed by sediment pulses (case 5).

Elevation data from the line laser were median-filtered on a rectangular grid to create DEMs and detrended for valley slope. DEMs of difference were calculated to assess morphological change and to identify erosional surfaces. Photographs were transformed to LAB color space to obtain water depth measurements from (red) rhodamine dye intensity. We used the luminosity (whiteness) and calibration samples to obtain silt cover maps (Fig. DR1, Van Dijk et al., 2013). Flow velocities were measured in selected bends by measuring track length of 4 mm floating polystyrene spheres on photographs with a fixed shutter speed of 0.10 seconds at a pixel resolution of 0.255 mm. Sequential digital elevation models of the meander morphology were used (42 DEMs included) to generate a synthetic stratigraphy, verified by lacquer peels, that records deposit age and erosional surfaces (Van de Lageweg et al., 2013). Lacquer peels are made by impregnating the final topography by a lacquer that penetrates some small distance and cements the grains together, so that a sedimentary deposit is preserved that can be pulled out from the experiment. The depth of thickness of the penetration depends on the permeability of the sediment. From the output location of the peel, virtual cores, transects and maps were constructed and analyzed. We qualitatively compared the synthetic slices to sediment peels that were made after the experiment.

Quantitative analysis

The effect of bar push and bank pull are quantified by measuring the displacement of the outer bank and inner bank compared to their initial location. Therefore, the selected bends were monitored with an overhead camera each 30 seconds. The displacement was quantified by plotting the coordinates of a bank located at the apex against time using successive photographs in Matlab. As result, the sensitivity of the location of the bend apex and the determined bank location leads to negative values for bends that hardly migrated, e.g., the static or fixed outer banks.

To predict the dip angle of lateral-accretion deposits ($\partial z/\partial n$) we used the theory of Struiksma et al. (1985, adapted by Talmon et al., (1995)), where n is the transverse coordinate in a curvilinear channel for damped conditions in an infinitely long bend:

$$\tan\left(\frac{\partial z}{\partial n}\right) = 9\left(\frac{D_{50}}{h}\right)^{0.3}\sqrt{\theta}\,\frac{2}{\kappa^2}\left(1-\frac{\sqrt{g}}{\kappa C}\right)\frac{h}{R} \qquad (1)$$

where θ = Shields mobility parameter ($\tau/((\rho_s-\rho)gD)$), κ = 0.4 Von Karman's constant, g = acceleration of gravity (9.81~ms^{-2}), 9 (D_{50}/h)0.3 = α and C = Chezy coefficient (here calculated as 18 log(12h/D_{90}). ∂z/∂n depends on α√θ and the helical flow strength (Struiksma et al., 1985). The water depth (h) was kept constant whilst bend radius (R) was varied. We compared this to the local curvature of the bend at the apex.

REFERENCES CITED

Lanzoni, S. and Seminara, G., 2006, On the nature of meander instability: Journal of Geophysical Research, v. 111, F04006.

Struiksma, N., Olesen, K.W., Flokstra, C. and De Vriend, H.J., 1985, Bed deformation in curved alluvial channels: Journal of Hydraulic Research, v. 23, p. 57–79.

Talmon, A., Struiksma, N. and Van Mierlo, M., 1995, Laboratory measurements of the direction of sediment transport on transverse alluvial-bed slopes: Journal of Hydraulic Research, v. 33, p. 495-517.

Van de Lageweg, W.I., Van Dijk, W.M. and Kleinhans, M.G., 2013, Channel belt architecture formed by an experimental meandering river: Sedimentology, v. 60, p. 840–859.

Van Dijk, W.M., Van de Lageweg, W.I. and Kleinhans, M.G., 2012, Experimental meandering river with chute cutoffs: Journal of Geophysical Research, v. 117, F03023.

Van Dijk, W.M., Van de Lageweg, W.I. and Kleinhans, M.G., 2013, Formation of a cohesive floodplain in a dynamic experimental meandering river: Earth Surface Processes and Landforms, v. 38, p. 1550-1565.

Figure DR1. Method to convert the whiteness of an image to a silt distribution map. a) True-color image draped on shaded DEM showing white silt on top of the point bar. b) Least-squares linear fit of differential luminosity (quantified by the image digital number (*dn*) on measured silt surface concentration (S_c). c) Silt cover map draped on shaded DEM.

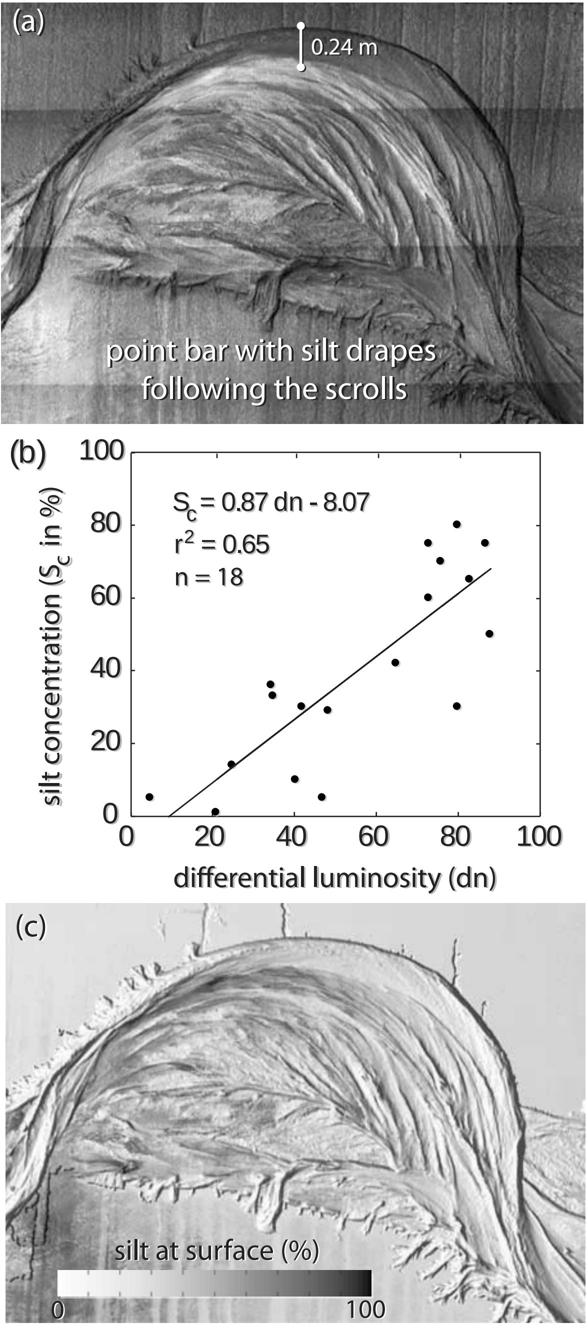

(a)
0.24 m
point bar with silt drapes following the scrolls
(b)
$S_c = 0.87\ dn - 8.07$
$r^2 = 0.65$
n = 18
silt concentration (S_c in %)
differential luminosity (dn)
0
20
40
60
80
100
(c)
silt at surface (%)
0
100